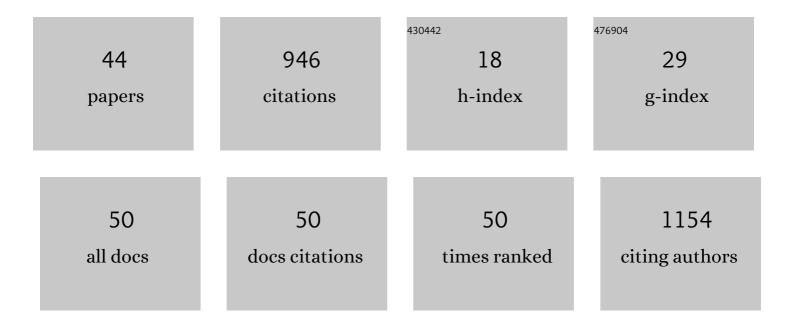
## Anna Rokicińska

List of Publications by Year in descending order

Source: https://exaly.com/author-pdf/1627643/publications.pdf Version: 2024-02-01



#	Article	lF	CITATIONS
1	Role of the Cu content and Ce activating effect on catalytic performance of Cu-Mg-Al and Ce/Cu-Mg-Al oxides in ammonia selective catalytic oxidation. Applied Surface Science, 2022, 573, 151540.	3.1	10
2	Lignin-Supported Heterogeneous Photocatalyst for the Direct Generation of H <sub>2</sub> O <sub>2</sub> from Seawater. Journal of the American Chemical Society, 2022, 144, 2603-2613.	6.6	80
3	Reaction pathways on N-substituted carbon catalysts during the electrochemical reduction of nitrate to ammonia. Catalysis Science and Technology, 2022, 12, 3582-3593.	2.1	6
4	Combustion of toluene over cobalt-modified MFI zeolite dispersed on monolith produced using 3D printing technique. Catalysis Today, 2021, 375, 369-376.	2.2	13
5	Sensibilization of <i>p</i> -NiO with ZnSe/CdS and CdS/ZnSe quantum dots for photoelectrochemical water reduction. Nanoscale, 2021, 13, 869-877.	2.8	8
6	Graphitic nitrogen in carbon catalysts is important for the reduction of nitrite as revealed by naturally abundant <sup>15</sup> N NMR spectroscopy. Dalton Transactions, 2021, 50, 6857-6866.	1.6	8
7	Combining Electrocatalysts and Biobased Adsorbents for Sustainable Denitrification. ACS Sustainable Chemistry and Engineering, 2021, 9, 3658-3667.	3.2	9
8	Tailoring Properties of Resol Resin-Derived Spherical Carbons for Adsorption of Phenol from Aqueous Solution. Molecules, 2021, 26, 1736.	1.7	5
9	Impact of Mn addition on catalytic performance of Cu/SiBEA materials in total oxidation of aromatic volatile organic compounds. Applied Surface Science, 2021, 546, 149148.	3.1	12
10	CeTiO <sub>2</sub> N oxynitride perovskite: paramagnetic <sup>14</sup> N MAS NMR without paramagnetic shifts. Zeitschrift Fur Naturforschung - Section B Journal of Chemical Sciences, 2021, 76, 275-280.	0.3	4
11	In Search of Factors Determining Activity of Co3O4 Nanoparticles Dispersed in Partially Exfoliated Montmorillonite Structure. Molecules, 2021, 26, 3288.	1.7	2
12	Design of Co3O4@SiO2 Nanorattles for Catalytic Toluene Combustion Based on Bottom-Up Strategy Involving Spherical Poly(styrene-co-acrylic Acid) Template. Catalysts, 2021, 11, 1097.	1.6	5
13	LignoPhot: Conversion of hydrolysis lignin into the photoactive hybrid lignin/Bi4O5Br2/BiOBr composite for simultaneous dyes oxidation and Co2+ and Ni2+ recycling. Chemosphere, 2021, 279, 130538.	4.2	21
14	Structural Properties of NdTiO2+xN1–x and Its Application as Photoanode. Inorganic Chemistry, 2021, 60, 919-929.	1.9	7
15	Selective Aerobic Oxidation of P-Methoxytoluene by Co(II)-Promoted NHPI Incorporated into Cross-Linked Copolymer Structure. Catalysts, 2021, 11, 1474.	1.6	3
16	Nanostructured core–shell metal borides–oxides as highly efficient electrocatalysts for photoelectrochemical water oxidation. Nanoscale, 2020, 12, 3121-3128.	2.8	29
17	Exploring the Origins of Improved Photocurrent by Acidic Treatment for Quaternary Tantalum-Based Oxynitride Photoanodes on the Example of CaTaO <sub>2</sub> N. Journal of Physical Chemistry C, 2020, 124, 152-160.	1.5	28
18	Semi-transparent quaternary oxynitride photoanodes on GaN underlayers. Chemical Communications, 2020, 56, 13193-13196.	2.2	16

Αννα Ροκιςιά,,, ska

#	Article	IF	CITATIONS
19	Metathetic synthesis of lead cyanamide as a p-type semiconductor. Dalton Transactions, 2020, 49, 14061-14067.	1.6	16
20	Electrochemical Denitrification and Oxidative Dehydrogenation of Ethylbenzene over N-doped Mesoporous Carbon: Atomic Level Understanding of Catalytic Activity by <sup>15</sup> N NMR Spectroscopy. Chemistry of Materials, 2020, 32, 7263-7273.	3.2	28
21	Tailoring the Surface Properties of Bi <sub>2</sub> O <sub>2</sub> NCN by <i>in Situ</i> Activation for Augmented Photoelectrochemical Water Oxidation on WO <sub>3</sub> and CuWO <sub>4</sub> Heterojunction Photoanodes. Inorganic Chemistry, 2020, 59, 13589-13597.	1.9	7
22	NiO/Poly(4-alkylthiazole) Hybrid Interface for Promoting Spatial Charge Separation in Photoelectrochemical Water Reduction. ACS Applied Materials & Interfaces, 2020, 12, 29173-29180.	4.0	7
23	Effect of support on the catalytic activity of Co3O4-Cs deposited on open-cell ceramic foams for N2O decomposition. Materials Research Bulletin, 2020, 129, 110892.	2.7	18
24	Increased photocurrent of CuWO <sub>4</sub> photoanodes by modification with the oxide carbodiimide Sn <sub>2</sub> O(NCN). Dalton Transactions, 2020, 49, 3450-3456.	1.6	14
25	Novel CuO-containing catalysts based on ZrO2 hollow spheres for total oxidation of toluene. Microporous and Mesoporous Materials, 2019, 279, 446-455.	2.2	26
26	Quaternary Core–Shell Oxynitride Nanowire Photoanode Containing a Hole-Extraction Gradient for Photoelectrochemical Water Oxidation. ACS Applied Materials & Interfaces, 2019, 11, 19077-19086.	4.0	35
27	Study on self-assembled monolayer of functionalized thiol on gold electrode forming capacitive sensor for chromium(VI) determination. Journal of Solid State Electrochemistry, 2019, 23, 1463-1472.	1.2	12
28	Photocatalytic hydrogen production from methanol over Nd/TiO2. Journal of Photochemistry and Photobiology A: Chemistry, 2018, 366, 55-64.	2.0	16
29	SrTaO <sub>2</sub> N Nanowire Photoanode Modified with a Ferrihydrite Hole-Storage Layer for Photoelectrochemical Water Oxidation. ACS Applied Nano Materials, 2018, 1, 869-876.	2.4	25
30	An MnNCN-Derived Electrocatalyst for CuWO <sub>4</sub> Photoanodes. Langmuir, 2018, 34, 3845-3852.	1.6	36
31	Photocatalytic decomposition of methanol over La/TiO2 materials. Environmental Science and Pollution Research, 2018, 25, 34818-34825.	2.7	23
32	Augmenting the Photocurrent of CuWO4 Photoanodes by Heat Treatment in the Nitrogen Atmosphere. Journal of Physical Chemistry C, 2018, 122, 19281-19288.	1.5	32
33	Polymer Hydrogel-Clay (Nano)Composites. Gels Horizons: From Science To Smart Materials, 2018, , 1-62.	0.3	2
34	Nd/TiO2 Anatase-Brookite Photocatalysts for Photocatalytic Decomposition of Methanol. Frontiers in Chemistry, 2018, 6, 44.	1.8	19
35	Abatement of Volatile Organic Compounds Emission as a Target for Various Human Activities Including Energy Production. Advances in Inorganic Chemistry, 2018, 72, 385-419.	0.4	33
36	TiO2 Processed by pressurized hot solvents as a novel photocatalyst for photocatalytic reduction of carbon dioxide. Applied Surface Science, 2017, 391, 282-287.	3.1	36

Αννα Ροκιςιά,,, ska

#	Article	IF	CITATIONS
37	Cobalt-containing BEA zeolite for catalytic combustion of toluene. Applied Catalysis B: Environmental, 2017, 212, 59-67.	10.8	91
38	Enhanced Photoelectrochemical Water Oxidation Efficiency of CuWO <sub>4</sub> Photoanodes by Surface Modification with Ag <sub>2</sub> NCN. Journal of Physical Chemistry C, 2017, 121, 26265-26274.	1.5	36
39	Enhancing Photoelectrochemical Water Oxidation Efficiency of WO <sub>3</sub> /αâ€Fe <sub>2</sub> O <sub>3</sub> Heterojunction Photoanodes by Surface Functionalization with CoPd Nanocrystals. European Journal of Inorganic Chemistry, 2017, 2017, 4267-4274.	1.0	23
40	Type A and B gelatin as precursors of silica-templated porous carbon with a specified number of nitrogen- and oxygen-containing functionalities. Materials Express, 2017, 7, 123-133.	0.2	3
41	Co3O4-pillared montmorillonite catalysts synthesized by hydrogel-assisted route for total oxidation of toluene. Applied Catalysis B: Environmental, 2016, 195, 59-68.	10.8	93
42	Physicochemical properties of hydrogel template-synthesized copper( <scp>ii</scp> ) oxide-modified clay influencing its catalytic activity in toluene combustion. RSC Advances, 2016, 6, 100373-100382.	1.7	7
43	MCM-41 modified with iron by template ion-exchange method as effective catalyst for DeNOx and NH 3 -SCO processes. Chemical Engineering Journal, 2016, 295, 167-180.	6.6	30
44	Hydrogel template-assisted synthesis of nanometric Fe 2 O 3 supported on exfoliated clay. Microporous and Mesoporous Materials, 2016, 221, 212-219.	2.2	12